Cell Host & Microbe, Volume *18*

Supplemental Information

Iron Regulatory Proteins Mediate Host Resistance to *Salmonella* Infection

Manfred Nairz, Dunja Ferring-Appel, Daniela Casarrubea, Thomas Sonnweber, Lydie Viatte, Andrea Schroll, David Haschka, Ferric C. Fang, Matthias W. Hentze, Guenter Weiss, and Bruno Galy

Figure S1

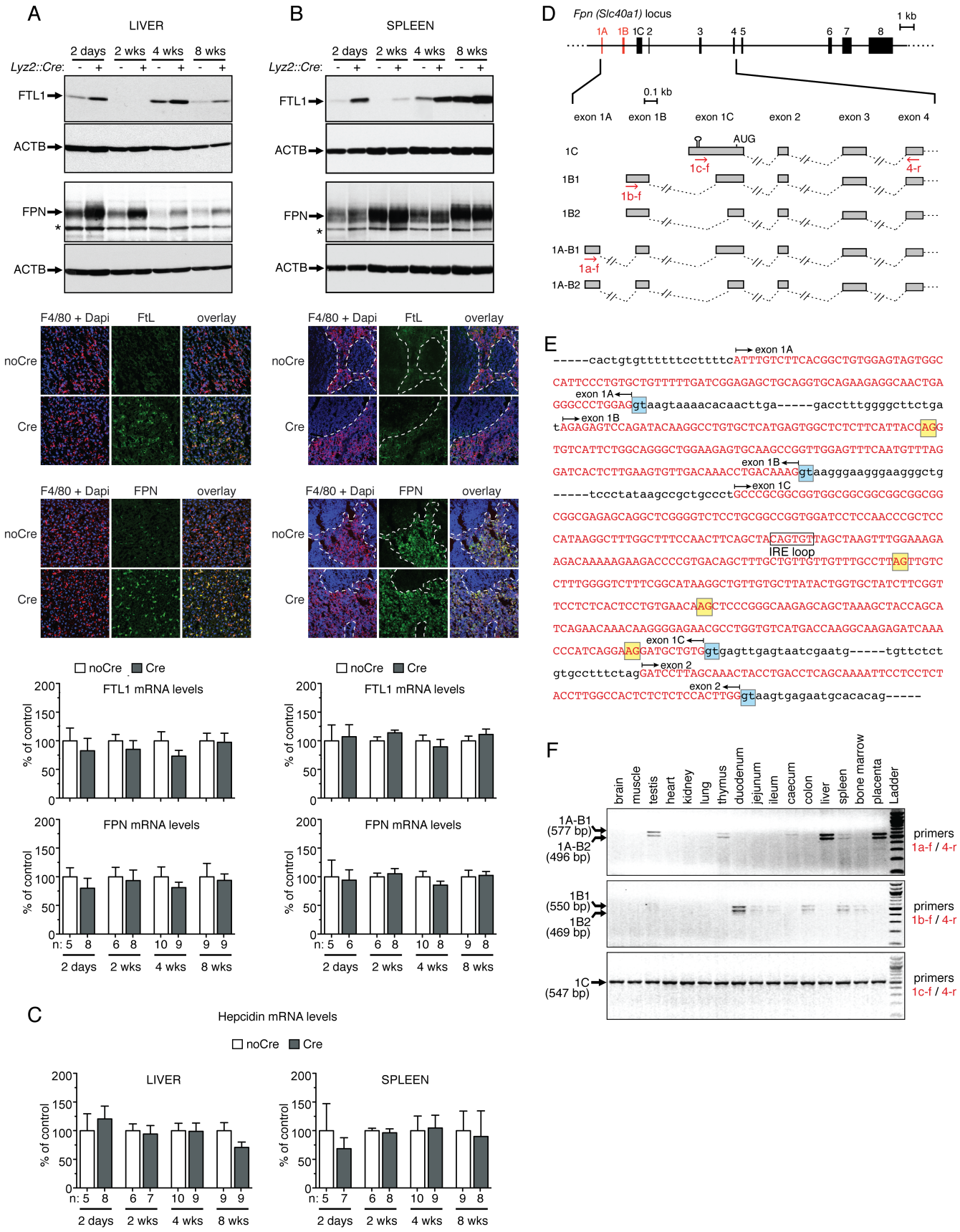
A
LIVER
2 days 2 wks 4 wks 8 wks
Lyz2::Cre: - + - + - + - +
FTL1
ACTB
FPN
*
ACTB
B
SPLEEN
2 days 2 wks 4 wks 8 wks
Lyz2::Cre: - + - + - + - +
FTL1
ACTB
FPN
*
ACTB
F4/80 + Dapi
FtL
overlay
noCre
Cre
F4/80 + Dapi
FtL
overlay
noCre
Cre
F4/80 + Dapi
FPN
overlay
noCre
Cre
F4/80 + Dapi
FPN
overlay
noCre
Cre
noCre Cre
FTL1 mRNA levels
% of control
FPN mRNA levels
% of control
n: 5 8 6 8 10 9 9 9
2 days 2 wks 4 wks 8 wks
noCre Cre
FTL1 mRNA levels
% of control
FPN mRNA levels
% of control
n: 5 6 6 8 10 8 9 8
2 days 2 wks 4 wks 8 wks
C
Hepcidin mRNA levels
noCre Cre
LIVER
% of control
n: 5 8 6 7 10 9 9 9
2 days 2 wks 4 wks 8 wks
SPLEEN
% of control
n: 5 7 6 8 10 9 9 8
2 days 2 wks 4 wks 8 wks
D
Fpn (Slc40a1) locus
1 kb
1A 1B 1C 2 3 4 5 6 7 8
0.1 kb
exon 1A exon 1B exon 1C exon 2 exon 3 exon 4
AUG
1C
1c-f
4-r
1B1
1b-f
1B2
1A-B1
1a-f
1A-B2
E
exon 1A
-----cactgtgtttttttcctttttcATTTGTCTTCACGGCTGTGGAGTAGTGGC
CATTCCCTGTGCTGTTTTTGATCGGAGAGCTGCAGGTGCAGAAGAGGCAACTGA
exon 1A
GGGCCCTGGAGgtaagtaaaacacaacttga-----gacctttggggcttctga
exon 1B
tAGAGAGTCCAGATACAAGGCCTGTGCTCATGAGTGGCTCTCTTCATTACCAGG
TGTCATTCTGGCAGGGCTGGAAGAGTGCAAGCCGGTTGGAGTTTCAATGTTTAG
exon 1B
GATCACTCTTGAAGTGTTGACAAACCTGACAAAGgtaagggaagggaagggctg
exon 1C
-----tccctataagccgctgccctGCCCGCGGCGGTGGCGGCGGCGGCGGCGG
CGGCGAGAGCAGGCTCGGGGTCTCCTGCGGCCGGTGGATCCTCCAACCCGCTCC
CATAAGGCTTTGGCTTTCCAACTTCAGCTACAGTGTTAGCTAAGTTTGGAAAGA
IRE loop
AGACAAAAAGAAGACCCCGTGACAGCTTTGCTGTTGTTGTTTGCCTTAGTTGTC
CTTTGGGGTCTTTCGGCATAAGGCTGTTGTGCTTATACTGGTGCTATCTTCGGT
TCCTCTCACTCCTGTGAACAAGCTCCCGGGCAAGAGCAGCTAAAGCTACCAGCA
TCAGAACAAACAAGGGGAGAACGCCTGGTGTCATGACCAAGGCAAGAGATCAAA
exon 1C
CCCATCAGGAAGGATGCTGTGgtgagttgagtaatcgaatg-----tgttctct
exon 2
gtgcctttctagGATCCTTAGCAAACTACCTGACCTCAGCAAAATTCCTCCTCT
ACCTTGGCCACTCTCTCTCCACTTGGgtaagtgagaatgcacacag-----
F
brain muscle testis heart kidney lung thymus duodenum jejunum ileum caecum colon liver spleen bone marrow placenta Ladder
1A-B1
(577 bp)
1A-B2
(496 bp)
primers
1a-f / 4-r
1B1
(550 bp)
1B2
(469 bp)
primers
1b-f / 4-r
1C
(547 bp)
primers
1c-f / 4-r

Figure S1, related to Figure 1: **Impact of IRP ablation on ferritin and FPN in tissue macrophages in vivo**. Protein and mRNA expression levels of ferritin and FPN were analyzed by western-blotting (upper panels) and qPCR (bottom histograms) in liver (A) and spleen (B) samples from $Irp^{LyzCre(-)}$ (noCre) versus $Irp^{LyzCre(+)}$ (Cre) mice at 2 days (newborn) as well as 2 (suckling pups), 4 (short after weaning) and 10 (adults) weeks of age, as indicated. β-actin (ACTB) was used as a loading control for western blotting. The middle panels in (A) and (B) show immuno-staining of ferritin and FPN (green color) in the liver and spleen of 8 week-old mice; macrophages are labeled with an anti-F4/80 antibody (red color), cell nuclei are stained with Dapi (blue color). Hepcidin mRNA expression was assessed in the same samples (C). qPCR data are displayed for each time point as percentage of control (i.e. $Irp^{LyzCre(-)}$ mice) after calibration to β-actin mRNA expression. Histograms display averages ± SEM. The number of mice (n) is indicated. No statistical difference in mRNA levels between Cre and noCre groups was observed (Student's t-test). $Irp^{LyzCre(+)}$ mice exhibit increased expression of both ferritin and FPN proteins in the liver throughout the time course of the study (A, top); tissue immunostaining confirmed selective ferritin and FPN upregulation in Kupffer cells (middle panels). This effect likely reflects increased translation as ferritin and FPN mRNA levels are not augmented (A, histograms). Ferritin is also posttranscriptionally upregulated in the spleen of IRP-mutant mice (B, top); although not as evident as in Kupffer cells, ferritin immunoreactivity is increased in F4/80 macrophages of the red pulp (delineated by a white dashed line) and in part in F4/80 negative cells (middles panels). However, FPN protein levels are unchanged (B, top and middle panels). The lack of FPN upregulation in IRP-deficient splenic macrophages is not due to a compensatory decrease in FPN mRNA levels (B, histograms) nor to *Hepcidin* stimulation in liver and spleen (C). D) Schematic representation of the murine *Fpn* locus (top) and the 5' variants of the FPN mRNA (bottom) identified by RACE (rapid amplification of cDNA ends). The exon containing the IRE motif (depicted as a stem loop) is named 1C. Additional variants are generated from upstream promoters. The variants named 1B1 and 1B2 contain exon 1B, which reacts with two alternative splice acceptor sites within exon 1C; similar isoforms have been reported previously (Zhang et al., 2009). Our RACE experiment reveals additional isoforms named 1A-B1 and 1A-B2; these isoforms contain exon 1A, which reacts with a single splice acceptor site within exon 1B. Because exon 1B reacts with splice acceptor sites located downstream the IRE in exon 1C, the 1A-B1, 1A-B2, 1B1 and 1B2 mRNA isoforms do not contain the IRE and escape IRP regulation. E) Sequence of the 5' exons (capital red letters) of the FPN mRNA as determined by RACE. The 10 nucleotides (small black letters) flanking each exon are indicated (gene assembly

ENSMUSG00000025993, Ensembl database, URL http://www.ensembl.org/index.html). Donor and acceptor splice sites are highlighted in blue and yellow, respectively. The IRE loop (CAGTGT) in exon 1C is indicated. F) The 5' FPN mRNA variants were analysed in mouse tissues by PCR using cDNA generated with random hexamers. The primer pairs used for PCR are indicated on the right and are depicted in (D); amplicon size is given in base pairs (bp). The 1C mRNA isoform bearing the IRE is very easily detected in all tissues, indicating relatively high expression. By contrast, the 1A-B1, 1A-B2, 1B1 and 1B2 isoforms are detected in a few tissues only. Moreover, more PCR cycles and longer image acquisition time were required to detect those isoforms, including in spleen, suggesting relatively low expression. This is in agreement with a previous report for the 1B1 and 1B2 isoforms (Zhang et al., 2009). These results indicate that the FPN mRNA variant carrying the IRE prevails. It is therefore unlikely that diversity in the FPN 5' mRNA leader fully explains why FPN protein levels remain unchanged in IRP-deficient splenic macrophages.

Figure S2

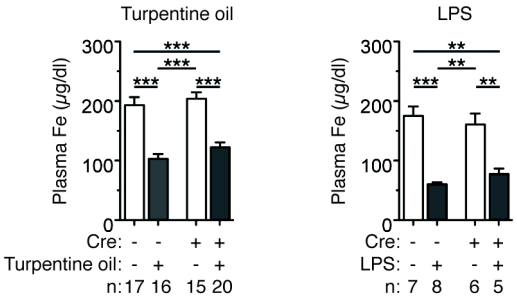

Figure S2, related to Figure 2: **Consequences of IRP ablation in macrophages on the hypoferremic response to aseptic inflammation**. 10-12-week old $Irp^{LyzCre(+)}$ (Cre) and $Irp^{LyzCre(-)}$ (noCre) littermates were exposed to sterile inflammatory stimuli that cause hypoferremia and stimulate hepcidin (Pigeon et al., 2001, Nicolas et al., 2002). Local and systemic inflammation was triggered, respectively, by injection of turpentine oil (Turp. oil) in the intrascapular fat pad or intraperitoneal injection of lipopolysaccharide (LPS); mice received vehicle as control. Plasma iron concentration was determined 18 hr (Turp. oil) or 8 hr (LPS) after injection. Data are given as average ± SEM. The sample size (n) is indicated. p: Student t-test (**: $p<0.01$; ***: $p<0.001$). Turpentine oil and LPS stimuli cause hypoferremia, as expected. $Irp^{LyzCre(+)}$ mice injected with LPS (and to a lesser extent with Turp. oil) tend to have slightly higher plasma iron levels than control littermates. This could possibly be due to abnormally high FPN expression in Kupffer cells. However the difference does not reach statistical significance. Overall these results show that the hypoferremic response to sterile inflammatory stimuli is largely preserved in mice lacking IRP expression in macrophages.

Figure S3

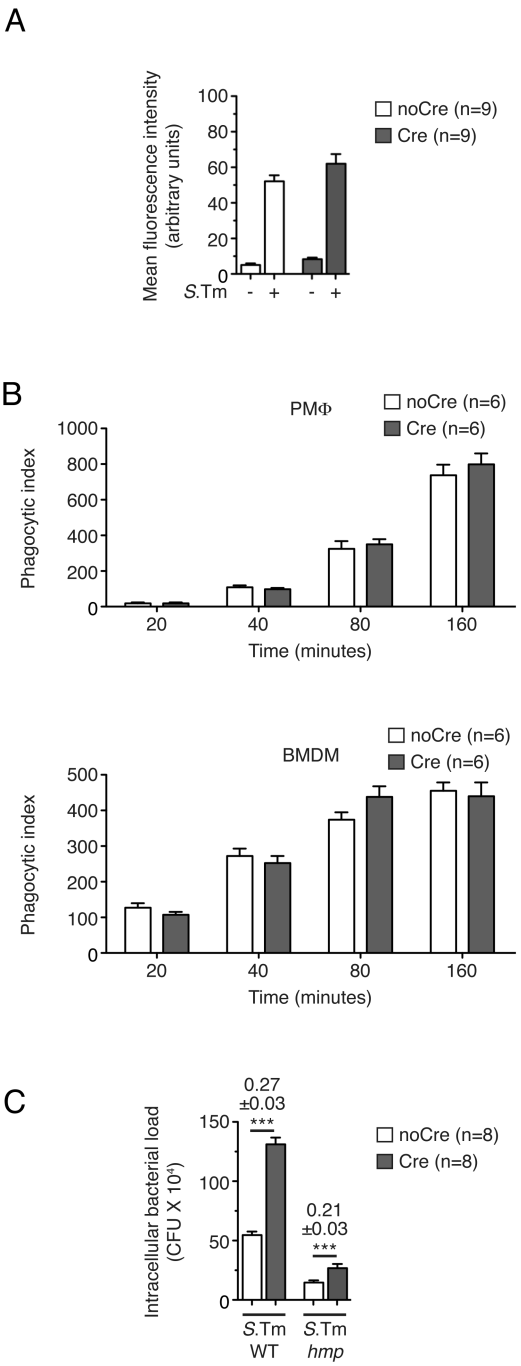

Figure S3, related to Figure 3: **Respiratory and phagocytic activity of macrophages lacking IRP expression and multiplication of flavohemoglobin mutant bacteria.** A) BMDMs from $Irp^{LyzCre(+)}$ (Cre) versus $Irp^{LyzCre(-)}$ (noCre) littermates were infected with *S*.Tm and ROS production was determined 4 hours later. ROS levels are expectedly increased in infected cells. $Irp^{LyzCre(+)}$ cells produce similar levels of ROS as $Irp^{LyzCre(-)}$ (Student's t-test), showing that the failure of IRP-deficient macrophages to combat *S*.Tm is not due to insufficient ROS production. B) PMΦ (top) and BMDMs (bottom) from $Irp^{LyzCre(+)}$ (Cre) versus

Irp$^{LyzCre(-)}$ (noCre) littermates were incubated with heat-killed *S.*Tm conjugated to a pH-sensitive fluorescent dye (pH-rodo^{TM}). Fluorescence is emitted when *S.*Tm particles are engulfed by the macrophages and encounter an acidic environment. Fluorescence emission was recorded over time by flow cytometry and the histograms display the phagocytic index (% of fluorescent cells X mean fluorescence / 100). The phagocytic indexes do not differ between control and IRP-mutant macrophages over the time course of the study (Student's t-test). These results show that differences in *S.*Tm proliferation in IRP-deficient versus control macrophages (Figures 3 and 4) are not related to basic alterations in macrophage phagocytic activity. C) *Irp*$^{LyzCre(+)}$ (Cre) and *Irp*$^{LyzCre(-)}$ (noCre) macrophages, respectively, were infected with a wild-type (*S.*Tm WT) or a flavohemoglobin-mutant (*S.*Tm *hmp*) *Salmonella* strain unable to detoxify reactive nitrogen species (RNS) produced by host cells (Bang et al., 2006). Multiplication of the *hmp S.*Tm mutant is expectedly reduced compared to wild-type bacteria. Yet, *Irp*$^{LyzCre(+)}$ macrophages remain significantly impaired in their antimicrobial activity towards the *hmp S.*Tm mutant (Student t-test, ***: $p<0.001$, the ratios above the bars indicate S.Tm proliferation in *Irp*$^{LyzCre(+)}$ versus *Irp*$^{LyzCre(-)}$ macrophages). These results suggest that reduced production of RNS (Figure 3D) is not the main mechanism underlying the antimicrobial deficit of *Irp*$^{LyzCre(+)}$. Data are presented as averages ± SEM. The sample size (n) is indicated.

Figure S4

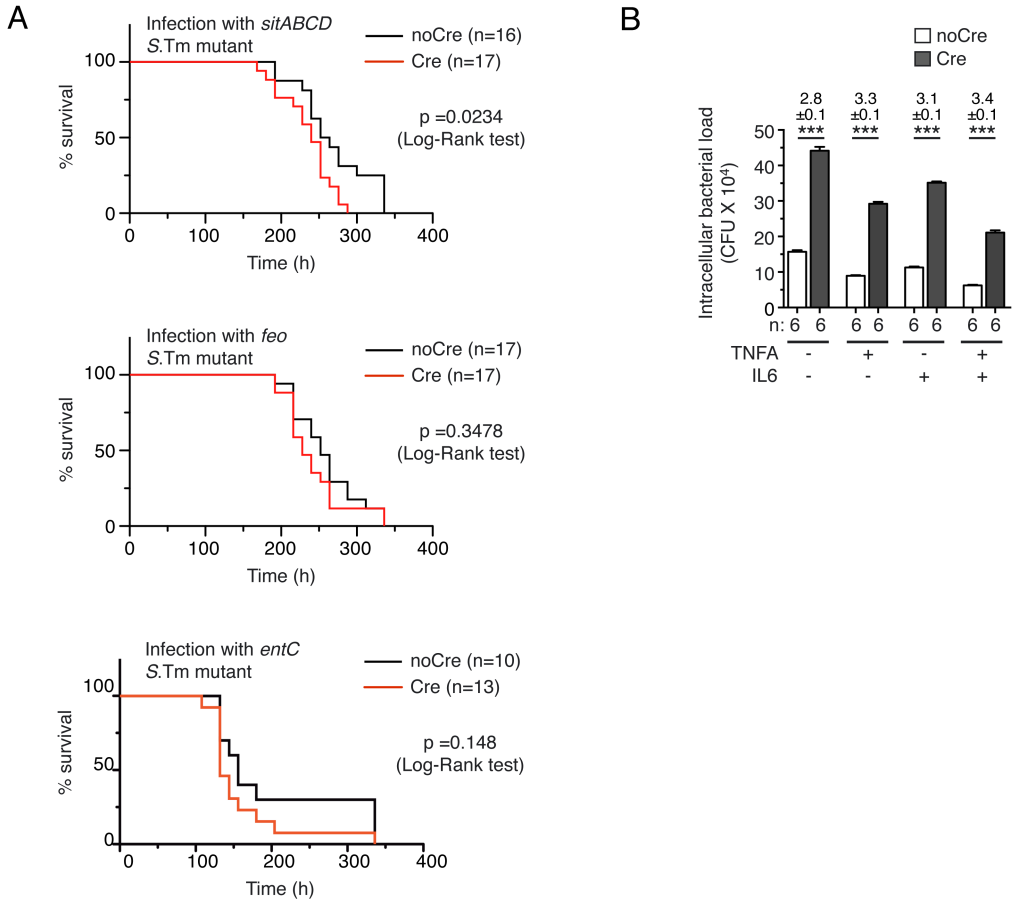

Figure S4, related to Figure 4: **Survival of mice infected with single *sitABCD*, *feo* or *entC Salmonella* mutants and role of TNFA and IL6 ex vivo**: A) $Irp^{LyzCre(+)}$ mice (Cre) and control littermates (noCre) were subjected to systemic infection (500 CFU) with mutant strains of *Salmonella* Typhimurium (*S*.Tm) deficient for either the *sitABCD* (top), the *feo* (middle), or the *entC* (bottom) iron uptake system, respectively. While $Irp^{LyzCre(+)}$ mice remain significantly more vulnerable to *sitABCD S*.Tm bacteria than $Irp^{LyzCre(+)}$ (p value < 0.05, long-Rank test), disruption of the *feo* and *entC* iron uptake systems, respectively, tend to abrogate the disadvantage conferred by macrophage IRP deficiency on mouse survival, mirroring the effect on intracellular bacterial proliferation observed in macrophages infected ex vivo. This indicates that macrophage IRPs target preferentially the bacterial *feo* and *entC* iron uptake systems but not *sitABCD* in vivo. Note that the amplitude of the phenotype is moderate compared to measurements of intracellular bacterial proliferation in isolated macrophages (see Fig. 4C); this discrepancy could possibly reflect the

influence of compensatory mechanisms at work in vivo but less active or absent in cultured macrophages. The sample size (n) is indicated). p: long-Rank test. B) Intracellular *S*.Tm proliferation in $Irp^{LyzCre(+)}$ (Cre) versus $Irp^{LyzCre(-)}$ (noCre) BMDMs infected in the presence of TNFA, IL6 or both cytokines; the ratios above the bars indicate the fold difference in intracellular bacterial growth in Cre versus noCre macrophages. TNFA and IL6, respectively, limit bacterial growth in both Cre and noCre BMDMs, and have an additive effect when added together. Unlike LCN2 (see Fig. 4C), those cytokines fail to revert the antimicrobial deficit of $Irp^{LyzCre(+)}$ cells. Hence, insufficient LCN2 production appears to play a dominant role in the antimicrobial deficit of IRP-deficient macrophages, at least ex vivo. The sample size (n) is indicated. p: Student's t-test (***: $p<0.001$).

Table S1, related to Figure 2: **Hematological parameters and tissue iron stores of mice lacking both IRP1 and 2 in macrophages**

	Males											
	2 days			2 weeks			4 weeks			8 weeks		
Hematology												
	noCre	Cre	p	noCre	Cre	p	noCre	Cre	p	noCre	Cre	p
	(5)	(7)		(6)	(9)		(13)	(13)		(11)	(9)	
WBC	4.3	4.7	0.78	10.1	11.0	0.67	11.2	10.8	0.85	13.3	11.2	0.28
10^9/L	±1.1	±0.8		±1.8	±1.2		±1.4	±0.9		±1.7	±0.7	
RBC	3.8	4.4	0.39	7.5	6.1	0.12	8.9	8.9	0.82	12.6	12.1	0.26
10^{12}/L	±0.3	±0.4		±0.7	±0.4		±0.1	±0.2		±0.3	±0.2	
Hb	15.7	17.2	0.57	11.5	10.2	0.33	14.7	14.7	0.94	18.8	18.1	0.39
g/L	±2.4	±1.0		±1.0	±0.9		±0.2	±0.3		±0.6	±0.4	
Hct	36.1	42.2	0.39	38.4	30.6	0.11	48.8	48.9	0.94	63.8	62.1	0.30
L/L	±4.5	±3.9		±3.5	±2.4		±0.4	±1.1		±1.2	±1.0	
MCV	93.2	95.0	0.30	51.2	49.9	0.34	54.8	54.8	0.95	51.9	52	0.80
fL	±1.5	±0.6		±0.5	±1.2		±0.3	±0.4		±0.3	±0.2	
Tissue iron							noCre	Cre	p	noCre	Cre	p
μg iron / mg dry tissue							(10)	(10)		(12)	(10)	
Spleen	nd			nd			327	316	0.73	1752	1550	0.32
							±27	±16		±176	±84	
							(10)	(9)		(11)	(9)	
Liver	nd			nd			267	273	0.84	221	191	0.18
							±13	±27		±19	±10	

	Females											
	2 days			2 weeks			4 weeks			8 weeks		
Hematology												
	noCre	Cre	p	noCre	Cre	p	noCre	Cre	p	noCre	Cre	p
	(6)	(7)		(10)	(11)		(9)	(12)		(13)	(10)	
WBC	5.4	4.4	0.09	12.4	15.1	0.47	10.0	11.5	0.37	13.6	12.2	0.30
10^9/L	±0.3	±0.4		±3.1	±1.7		±0.9	±1.2		±1.0	±0.8	
RBC	4.7	4.1	0.24	7.8	6.9	0.16	9.4	9.3	0.75	11.5	11.2	0.44
10^{12}/L	±0.3	±0.4		±0.5	±0.4		±0.2	±0.1		±0.2	±0.3	
Hb	17.5	15.9	0.21	12.8	11.7	0.40	15.5	15.4	0.86	17.6	17.2	0.41
g/L	±0.9	±0.7		±0.8	±0.9		±0.3	±0.3		±0.3	±0.4	
Hct	45.6	38.5	0.18	41.1	36.4	0.26	51.1	50.3	0.58	60.9	59.2	0.31
L/L	±3.5	±3.6		±3.3	±2.3		±1.1	±0.7		±0.8	±1.3	
MCV	96.5	94.7	0.25	51.8	53.3	0.38	53.6	54.3	0.69	53.2	52.8	0.44
fL	±1.2	±0.8		±1.3	±1.0		±0.6	±0.3		±0.3	±0.3	

Tissue iron			noCre	Cre	p	noCre	Cre	p
*μ*g iron / mg dry tissue			(9)	(10)		(12)	(10)	
Spleen	nd	nd	418	469	0.33	2517	2647	0.67
			±31	±40		±170	±242	
			(7)	(7)		(12)	(12)	
Liver	nd	nd	381	347		349	369	0.51
			±9	±17		±25	±21	

The hematological parameters of $Irp^{LyzCre(+)}$ (Cre) versus $Irp^{LyzCre(-)}$ (noCre) littermates were determined at 2 days as well as 2, 4 and 8 weeks of age, as indicated. Iron levels in spleen and liver tissues were determined at 4 and 8 weeks of age, respectively, but not at earlier developmental stages (indicated nd) due to limitation in tissue size. Data are given as average ± SEM. The sample size is indicated in parentheses. p: Student t-test, comparison between noCre and Cre within each age group.

These results indicate that IRP ablation in macrophages does not have a major impact on systemic iron parameters under standard laboratory conditions.

Supplemental Experimental Procedures

Mice. 2-day-old neonates were sacrificed by decapitation to collect trunk blood and organs; 2- and 4-week-old and adult mice were euthanised by CO_2 inhalation to collect blood by cardiac puncture and organs. Aseptic local inflammation was produced by a single injection of turpentine oil (0.1 ml/20 g of body weight, Sigma-Aldrich, Taufkirchen, Germany) into the intrascapular fat pad of 10- to 12-week old $Irp^{LyzCre(+)}$ versus $Irp^{LyzCre(-)}$ mice (Viatte et al., 2009). As control, mice received the same volume of saline solution (0.9% NaCl). The animals were sacrificed 18 hr later for blood collection. Sterile, systemic inflammation was triggered by a single injection (i.p.) of lipopolysaccharide (Sigma-Aldrich) at a dose of 2.5 μg/g body weight versus the same volume of vehicle; blood was collected 8 hr later for measurement of plasma iron concentration.

Blood iron parameters. Red blood cell profiles and hemoglobin content were determined using the ABC Vet apparatus (ABX Diagnostics, Montpellier, France). Plasma iron and unbound iron binding capacity (UIBC) were assayed using the Iron SFBC and Iron UIBC kits (Biolabo, Maizy, France) and plasma ferritin concentration was determined using an Olympus 400 analyzer as described (Galy et al., 2013).

Total non-heme iron levels. Liver and spleen tissues samples were dried and their non-heme iron content was measured using the bathophenanthroline method as described (Galy et al, 2005). To determine cellular iron levels, BMDMs were lysed in 50 mM NaOH and the iron content was measured using the ferrozine chromophore as described (Riemer et al., 2004). The results were calibrated to the protein content as determined with the Dc protein assay (Biorad, Munich, Germany).

RNA analysis. Total RNA extraction, reverse transcription (RT), and quantitative real-time PCR (qPCR) were performed as described previously (Galy et al., 2013). The primers used for qPCR are listed below.

Protein analysis. Tissue and cell lysates were prepared as described previously (Ferring-Appel et al., 2009). Immunoblotting was performed using the antibodies listed below.

Flow cytometry analysis of macrophage phagocytic activity. Heat-killed *S*.Tm were labeled with pHrodo-dye (Life technologies GmbH) according to manufacturer's instructions. BMDMs and PMΦ were incubated with 0.1 mg of pHrodo-S.Tm at 37°C for 20, 40, 80, or 160 min, respectively. Cells were subsequently washed with PBS, dislodged and their fluorescence measured by flow cytometry; DNA staining with DAPI (0.2 ng/ml) was used to exclude dead cells. The flow cytometry analysis was performed with a BD LSRFortessa™ cell analyzer (BD Biosciences, Heidelberg, Germany) together with the Flow-Jo software (Tree Star, Ashland, OR). To determine the auto-fluorescence of pHrodo-*S*.Tm particles attached to the cell surface, macrophages were incubated with pHrodo-*S*.Tm for 5 min only and used to gate negative cells. As negative control, the phagocytosis assay was performed in the presence of 10nM of the actin-polymerization inhibitor Cytochalasin D (Sigma-Aldrich). Each condition was assayed in duplicate and the average of the duplicates was used for subsequent calculations. Macrophages were obtained from six $Irp^{LyzCre(+)}$ versus six $Irp^{LyzCre(-)}$ mice.

Cytokine and NO assays. Specific ELISA kits were used to determine the concentration of TNFA, IL6, IL1β, IL12, IL10 (BD Biosciences, Heidelberg, Germany) and LCN2 (R&D Systems GmbH) in cell culture supernatants. Determination of nitrite, an oxidation product of NO, was carried out using the Griess reagent (Merck Millipore, Darmstadt, Germany).

Determination of reactive oxygen species (ROS) production. BMDMS from $Irp^{LyzCre(+)}$ versus $Irp^{LyzCre(-)}$ mice were seeded onto 6-well plates and infected with S.Tm at a MOI of 20. 4 hours after infection, ROS were detected using the fluorigenic CellROX® Deep Red Reagent (Life technologies GmbH, Darmstadt, Germany) together with a Gallios™ TM flow cytometer (Beckman Coulter, Vienna, Austria); dead cells were excluded from the analysis after staining with the SYTOX® Dead Cell Stain (Life technologies GmbH).

Macrophage treatment with TNFA and/or IL6. Macrophages were infected with *S*.Tm at a MOI of 10 in the presence of IL6 (10 ng/ml, R&D Systems GmbH) and/or TNFA (10 ng/ml, R&D Systems GmbH) in the culture medium and intracellular bacterial multiplication was determined as described previously (Nairz et al., 2013).

***hmp* mutant bacterial strain.** The flavohemoglobin *S*.Tm mutant strain is an isogenic derivative of the *S*. Tm wild-type strain ATCC 14028s. The strain was constructed and grown as described (Bang et al., 2006).

Bacterial load determination in liver and spleen. The bacterial load was determined by plating serial dilutions of organ homogenates on LB agar (Sigma-Aldrich) under sterile conditions and the number of bacteria was calculated per gram of tissue as previously described (Nairz et al., 2013).

5'RACE. RACE was performed using total RNA from mouse spleen and the FirstChoice® RLM-RACE kit (Life technologies GmbH) following the instructions of the manufacturer. The PCR products obtained were subcloned into the pCR4®-TOPO TA cloning vector (Life technologies GmbH) for DNA sequencing. See below the sequence of FPN mRNA primers used for RACE.

Antibodies used for immunoblotting Mouse monoclonal anti beta-ACTIN (clone AC15, Sigma-Aldrich) used 1/5000 in TBST (10 mM Tris pH8.0, 150 mM NaCl, 0.2% Tween20) + 5% dry milk.

Rabbit polyclonal anti-FPN/SLC40A1 (MTP11-A, Acris Antibodies GmbH, Herford, Germany), used 1 μg/ml in TBST + 5% dry milk.

Goat polyclonal anti-Ferritin L (sc-14420, Santa Cruz Biotechnology, Heidelberg, Germany), used 1/500 in TBST + 5% dry milk.

Goat polyclonal anti-Ferritin H (sc-14416, Santa Cruz Biotechnology), used 1/200 in TBST + 5% dry milk.

Mouse monoclonal anti-TFRC (clone H68.4, Life technologies GmbH), used 1/1000 in TBST + 5% dry milk.

Self-made rabbit polyclonal antibodies against IRP1 versus IRP2 (Galy, 2005b), used 1/500 in TBST + 5% dry milk.

Tissue immunostaining

Tissue sections (10 μm) were prepared on cryostat (model CM3050; Leica Microsystems, Wetzlar, Germany) and fixed in methanol or in acetone, respectively, for detection of FPN and ferritin. Proteins of interest were detected using the following primary antibodies: rabbit polyclonal anti-ferritin L (F6136,

Sigma, used 1/250), self-made rabbit polyclonal antibody against FPN (Galy, 2005b, used 1/250) and rat monoclonal anti-F4/80 (MCA497, AbD Serotec, Puchheim, Germany, used 1/250). Fluorescently-labeled secondary antibodies were: goat anti-rat coupled to Alexa Fluor 594 (A11007, Life technologies GmbH, used 1/500), and goat anti-rabbit coupled to Alexa Fluor 488 (A11008, Life technologies GmbH, used 1/500). Signal specificity was assessed by replacing primary antibodies with the corresponding normal sera, or by using competing peptides when available (FPN). Nuclei were stained with 4,6 diamidino-2-phenylindole (Dapi, Life technologies GmbH). Samples were mount in Fluoromount-G (BIOZOL Diagnostica Vertrieb GmbH, Eching, Germany). Images were acquired under a DMIRE2 confocal microscope equipped with a 40X oil-objective (NA 1.25) using the Leica confocal software (Leica Microsystems). Final pictures were prepared using the Fiji open-source image processing software (Schindelin et al., 2012).

Bacterial ^{59}Fe uptake. PMΦ were seeded in complete RPMI free of antibiotics and infected with *S.*Tm at a MOI of 10. Thereafter, cells were washed three times with PBS and incubated in serum-free HEPES-buffered RPMI containing 20 μg/ml gentamicin and 5 µM ^{59}Fe-citrate (PerkinElmer LAS GmbH, Rodgau, Germany). After 4 hours, macrophages were lysed in 0.1% SDS complemented with 10,000 U/ml DNase-I (Life technologies GmbH) and a EDTA-free protease inhibitor cocktail (Roche, Mannheim, Germany) to release intracellular bacilli. After 10 min incubation at room temperature (RT), a fraction of the lysate was used to measure total radioactivity and the rest was centrifuged at 10,000 g for 10 min (RT) to pellet the released bacilli. The bacterial pellet was washed three times with RPMI containing 0.01% SDS and 1 mg/ml proteinase K (Roche) and resuspended in the same solution after the final wash. 1/10th of the sample was plated in serial dilutions onto agar plates to determine the number of released bacteria, the rest was filtered through 0.22 μm PDVF spin columns (Merck Millipore). The filters containing the trapped bacteria were washed five times with 0.9% NaCl and the amount of *S.*Tm-associated ^{59}Fe was assessed using a LKB 1272 CliniGamma γ-counter (Wallac, Turku, Finland). The amount of *S.*Tm-associated ^{59}Fe was normalized to the number of bacteria

Determination of ferritin- versus *S.*Tm-associated ^{59}Fe. BMDMs were incubated in serum-free HEPES-buffered RPMI containing 5 μM ^{59}Fe-citrate (PerkinElmer LAS GmbH) for 12 hours. Cells were subsequently infected with *S.*Tm (MOI 10) for 12 hours, or left untreated. After extensive washes with

0.9% NaCl cells were lysed in NET buffer (150 mM NaCl, 10 mM EDTA, 10 mM Tris, pH 7.4) containing 0.1% Triton X-100 (Sigma-Aldrich). Samples were split in 3 aliquots to determine, respectively, the bacterial load (serial dilutions onto agar plates) and the relative amount of ^{59}Fe associated with *S.*Tm versus ferritin. To measure *S.*Tm-associated ^{59}Fe, lysates were treated with proteinase K and Dnase I (Life technologies GmbH) and filtered through a 0.22 μm PDVF spin column (Merck Millipore). To determine the amount of ^{59}Fe associated with ferritin, lysates were complemented with a EDTA-free protease inhibitor cocktail (Roche) and ferritin immunoprecipitation was performed using a rabbit human-Ft antibody together with a protein G immunoprecipitation kit (both from Sigma-Aldrich) according to the manufacturer's instructions. The ^{59}Fe radioactivity associated with PDVF membranes or protein G agarose beads was measured in a γ-counter as described above. The amount of *S.*Tm-associated radioactivity was normalized to the number of bacteria.

List of primers used for qPCR

- TFRC

forward 5'-CCCATGACGTTGAATTGAACCT-3'

reverse 5'-GTAGTCTCCACGAGCGGAATA-3'

- FPN/SLC40A1

forward 5'-GGGTGGATAAGAATGCCAGACTT-3'

reverse 5'-GTCAGGAGCTCATTCTTGTGTAGGA-3'

- Ferritin L

forward 5'-CGTGGATCTGTGTCTTGCTTCA-3'

reverse 5'-GCGAAGAGACGGTGCAGACT-3'

- Ferritin H

forward 5'-TGGAACTGCACAAACTGGCTACT-3'

reverse 5'-ATGGATTTCACCTGTTCACTCAGATAA -3'

- ACTB (beta-actin)

forward 5'-CAGGCATTGCTGACAGGATGCA-3'

reverse 5'-GGCCAGGATGGAGCCACCGATC-3'

- Hepcidin/Hamp

forward 5'-CCTATCTCCATCAACAGAT-3'

reverse 5’-TGCAACAGATACCACACTG-3’

- TUBB5 (tubulin)

forward 5’-GGGAAATCGTGCACATCCA-3’

reverse 5’-ATGCCATGTTCATCGCTTATCA-3’

- TNFA

forward 5’-TCTTCTCATTCCTGCTTGTGG-3’

reverse 5’-GGTCTGGGCCATAGAACTGA-3’

- IL6

forward 5’-GCTACCAAACTGGATATAATCAGGA-3’

reverse 5’-CCAGGTAGCTATGGTACTCCAGAA-3’

-IL1B

forward 5’-AGTTGACGGACCCCAAAAG-3’

reverse 5’-TTTGAAGCTGGATGCTCTCAT-3’

- IL12-p35

forward 5’-GTTTACCACTGGAACTACACAAGAAC-3’

reverse 5’-CAGGGTCATCATCAAAGACG-3’

- IL10

forward 5’-CAGAGCCACATGCTCCTAGA-3’

reverse 5’-GTCCAGCTGGTCCTTTGTTT-3’

- LCN2

forward 5’-CCATCTATGAGCTACAAGAGAACAAT-3’

reverse 5’-TCTGATCCAGTAGCGACAGC-3’

List of primers used for 5’RACE and PCR detection of FPN mRNA variants

- primers for RACE

Outer FPN RACE primer (reverse) 5’-AGTCCATGCGACAGCTGTCAAG-3’

Nested FPN RACE primer (reverse) 5’-TGAGGTCAGGTAGTTTGCTAAG-3’

- primers for PCR detection of FPN mRNA variants in mouse tissues

1a-f 5’- TGCAGGTGCAGAAGAGGCAACTG-3’ (forward primer in exon 1a).

1bf 5’- ATTACCAGGTGTCATTCTGGCAGG-3’ (forward primer in exon 1b downstream the splice acceptor site).

1c-f 5’- TTGGCTTTCCAACTTCAGCTACAGTG-3’ (forward primer in exon 1C partially overlapping with the IRE).

4-r 5’- ACGGACACATTCTGAACCACCAG-3’ (reverse primer in exon 4)

Supplemental References

Bang, L.S., Liu, L., Vazques-Torres, A., Crouch, M.L., Stamler, J.S., and Fang, F.C. (2006). Maintenance of nitric oxide and redox homeostasis by the *Salmonella* flavohemoglobin Hmp. J. Biol. Chem *281*:28039-28047.

Galy, B., Ferring, D., Minana, B., Bell, O., Janser, H.G., Muckenthaler, M., Schümann, K., and Hentze, M.W. (2005b). Altered body iron distribution and microcytosis in mice deficient in iron regulatory protein 2 (IRP2). Blood *106*, 2580-2589.

Nicolas, G., Chauvet, C., Viatte, L., Danan, J.L., Bigard, X., Devaux, I., Beaumont, C., Kahn, A., and Vaulont, S. (2002). The gene encoding the iron regulatory peptide hepcidin is regulated by anemia, hypoxia, and inflammation. J. Clin. Invest. *110*, 1037-1044.

Pigeon, C., Ilyin, G., Courselaud, B., Leroyer, P., Turlin, B., Brissot, P., and Loréal, O. (2001) A new mouse liver-specific gene, encoding a protein homologous to human antimicrobial peptide hepcidin, is overexpressed during iron overload. J. Biol. Chem. *276*, 7811-7819.

Riemer, J., Hoepken, H.H., Czerwinska, H., Robinson, S.R., and Dringen, R. (2004). Colorimetric ferrozine-based assay for the quantitation of iron in cultured cells. Anal. Biochem. *331*,370-375.

Schindelin, J., Arganda-Carreras, I., Frise, E., Kaynig, V., Longair, M., Pietzsch, T., Preibisch, S., Rueden, C., Saalfeld, S., Schmid, B., et al. (2012) "Fiji: an open-source platform for biological-image analysis" Nat. Methods *9*, 676-682.

Viatte, L., Gröne, H.J., Hentze, M.W., and Galy, B. (2009). In vivo role(s) of the iron regulatory proteins (IRP) 1 and 2 in aseptic local inflammation. J. Mol. Med. (Berl). *87*, 913-921.

Zhang, D.L., Hughes, R.M., Ollivierre-Wilson, H., Ghosh, M.C., and Rouault, T.A. (2009). A ferroportin transcript that lacks an iron-responsive element enables duodenal and erythroid precursor cells to evade

translational repression. Cell Metab. *9*, 461-473.